

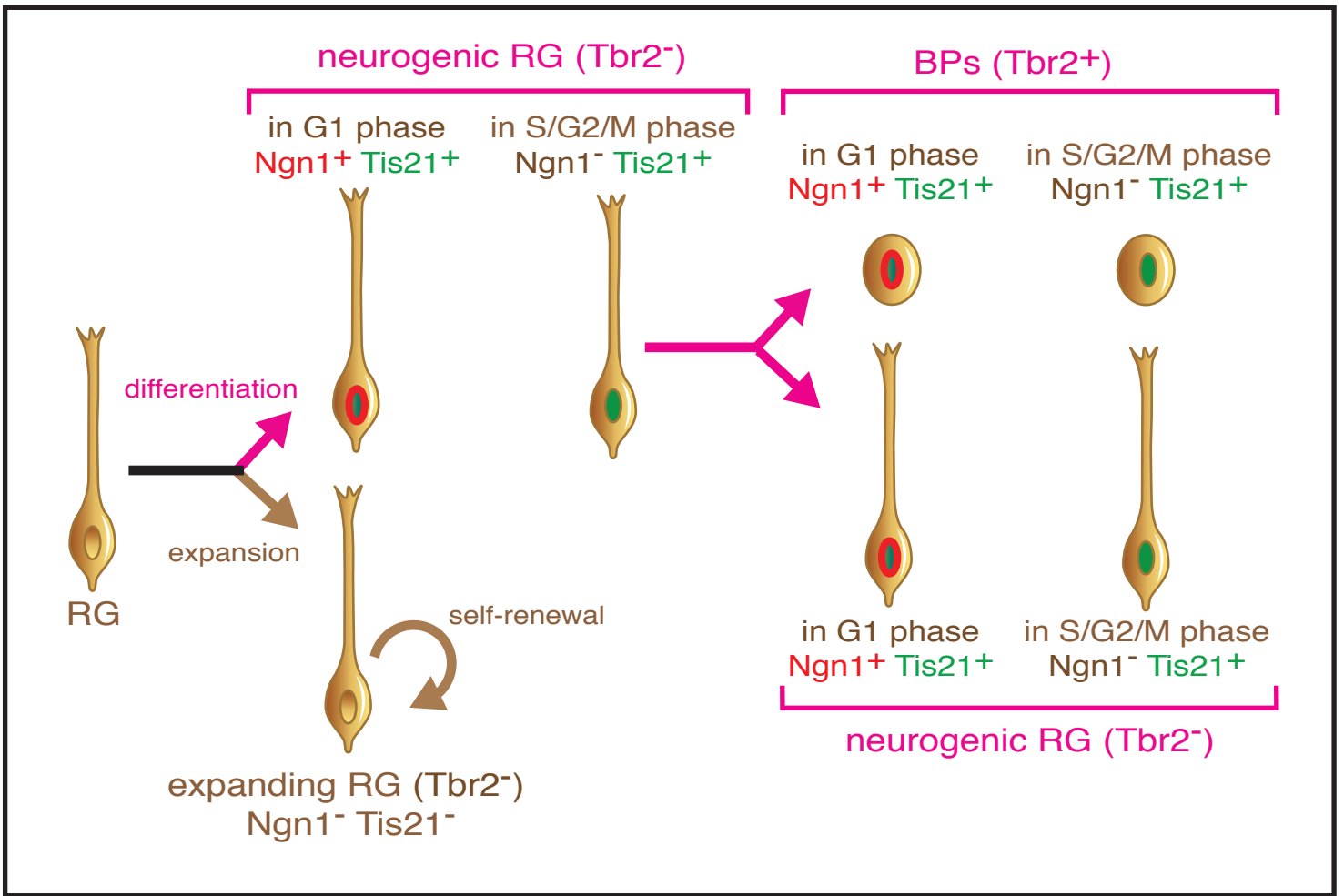
## **APPENDIX**

**5 APPENDIX FIGURES**

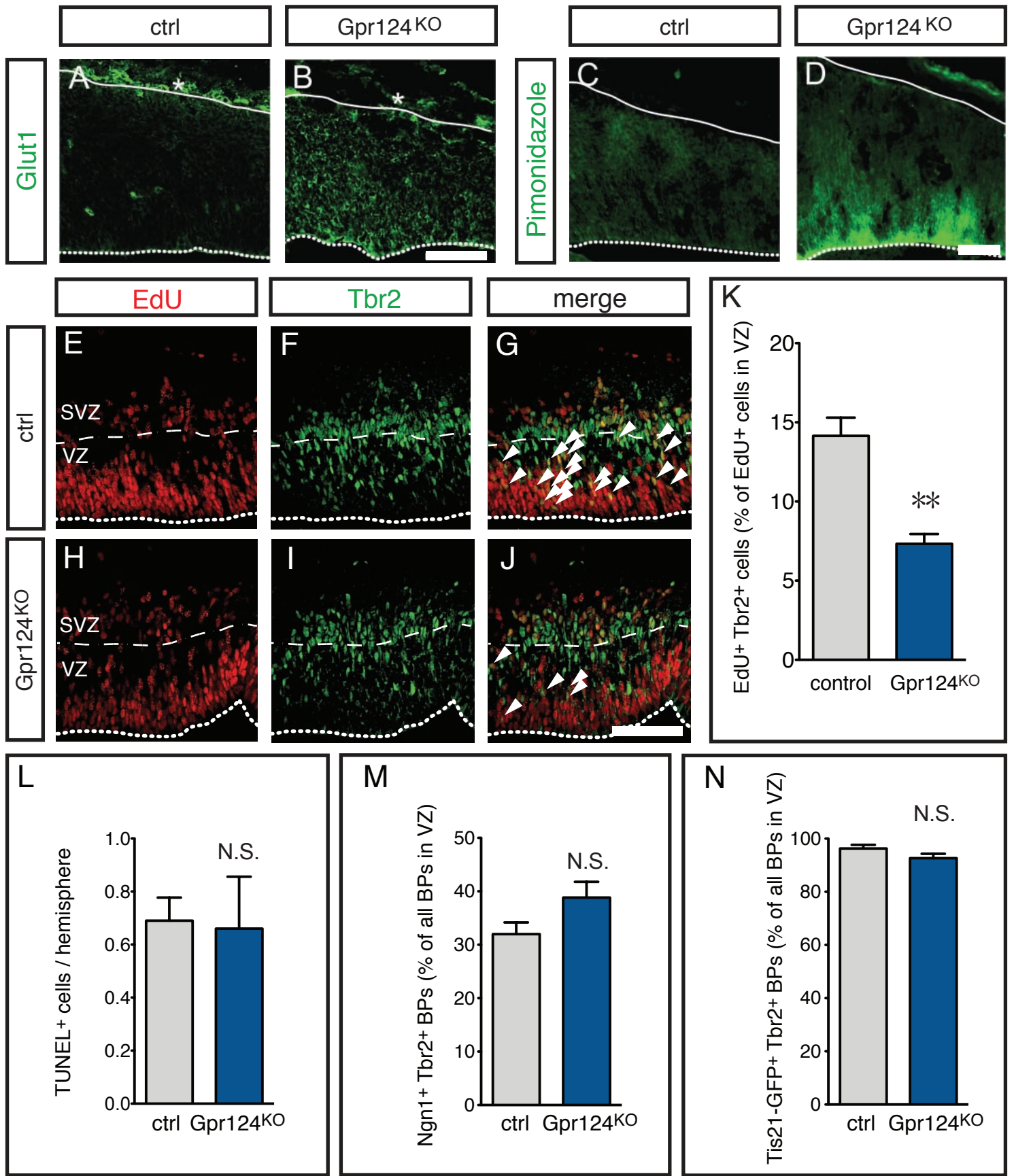
**APPENDIX FIGURE LEGENDS**

**APPENDIX SUPPLEMENTAL MATERIALS AND METHODS**

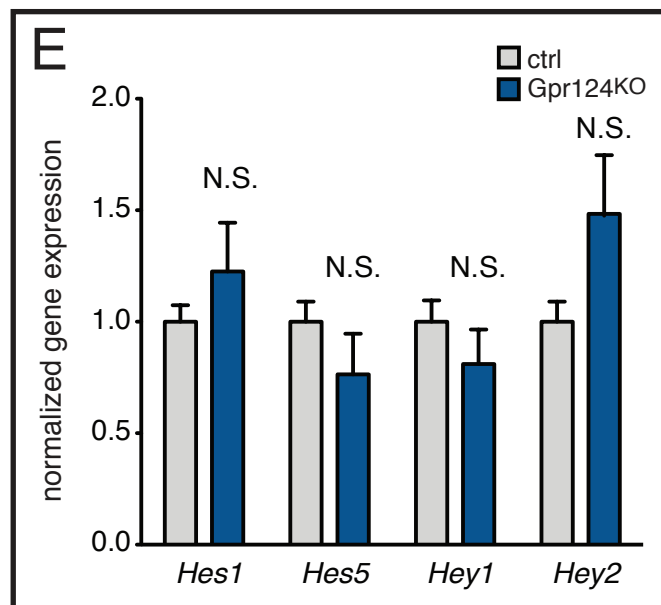
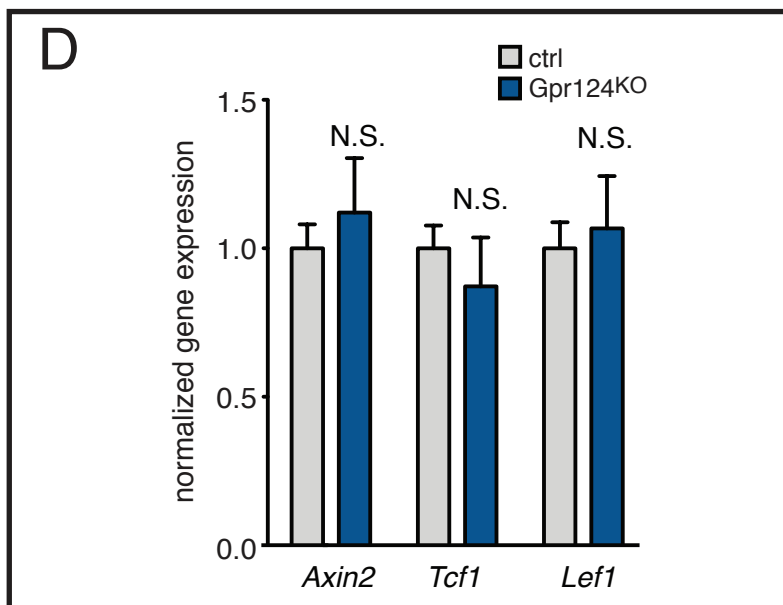
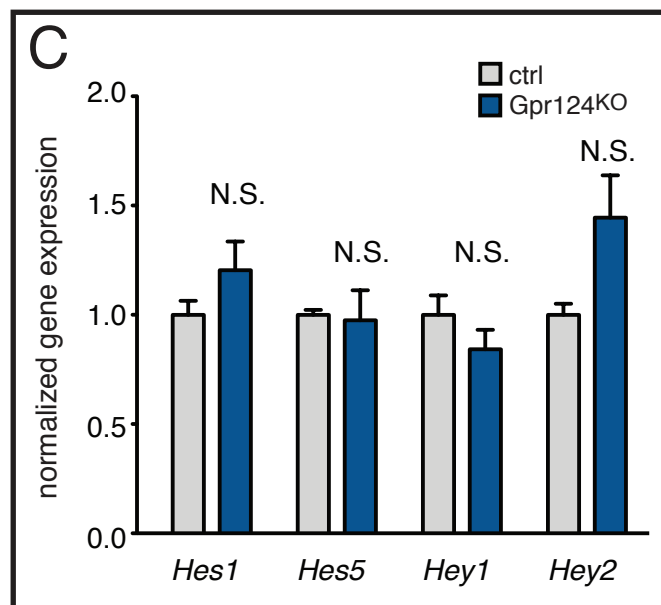
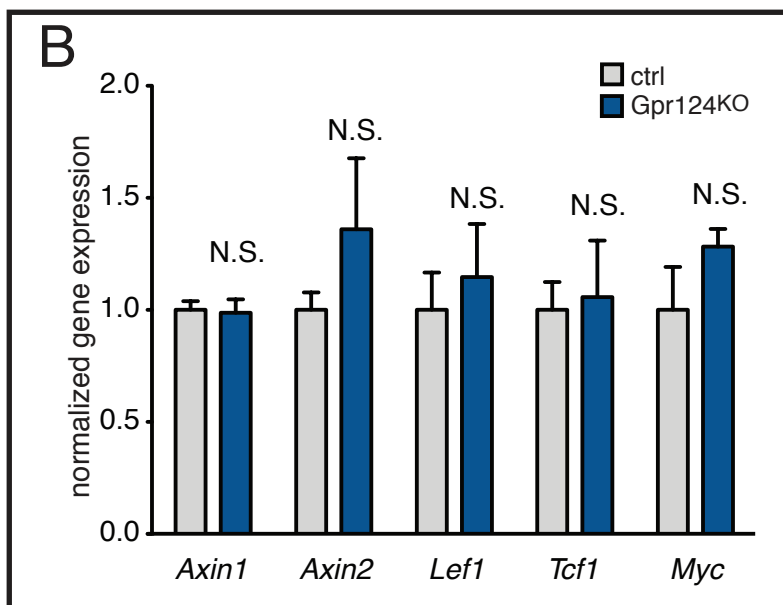
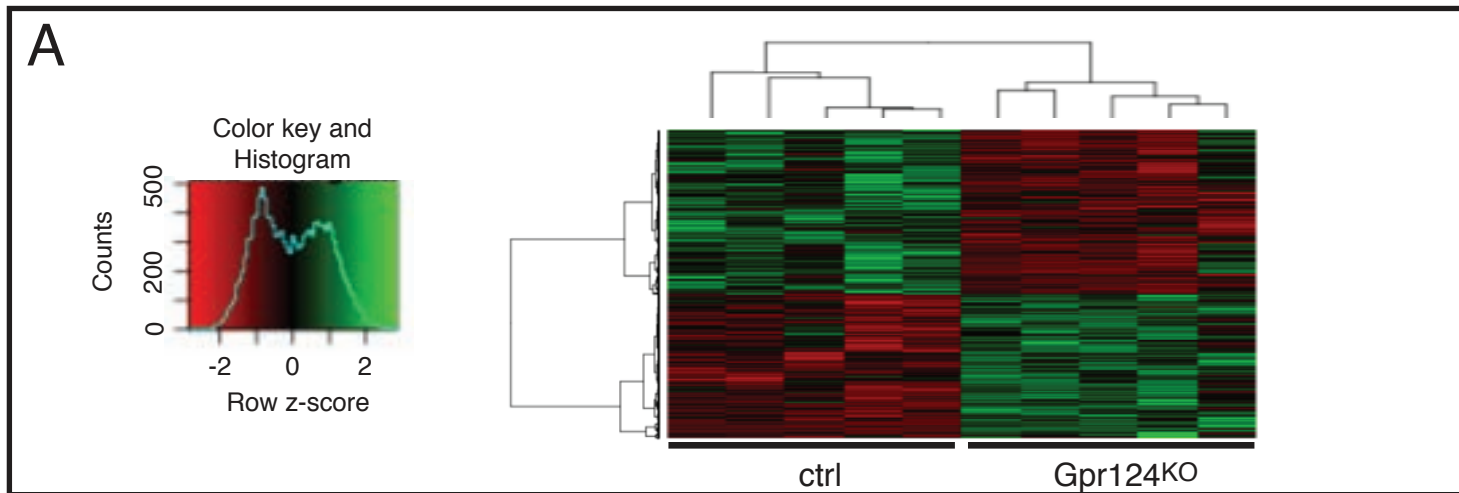
**1 APPENDIX TABLE**



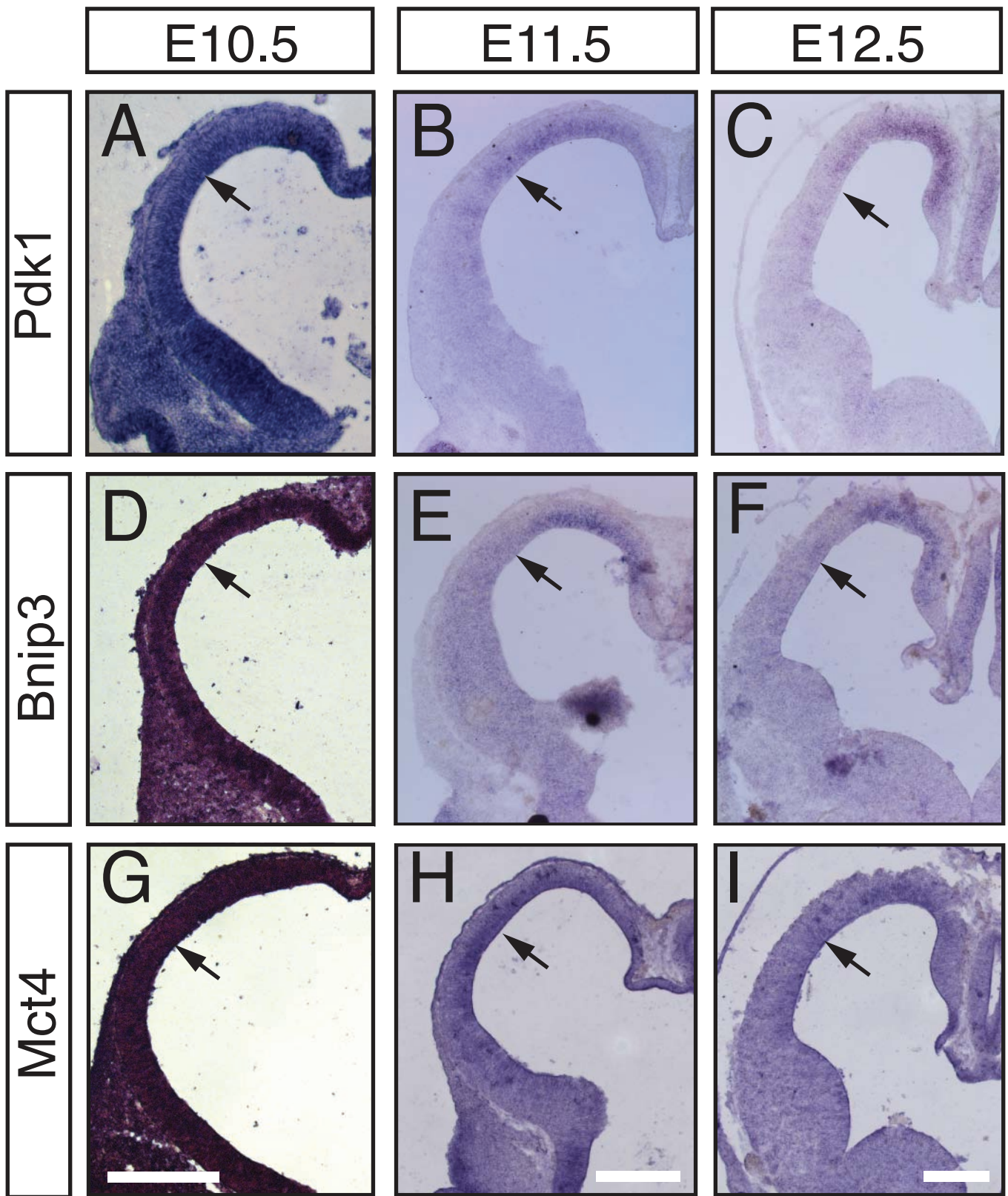
Appendix Figure S1



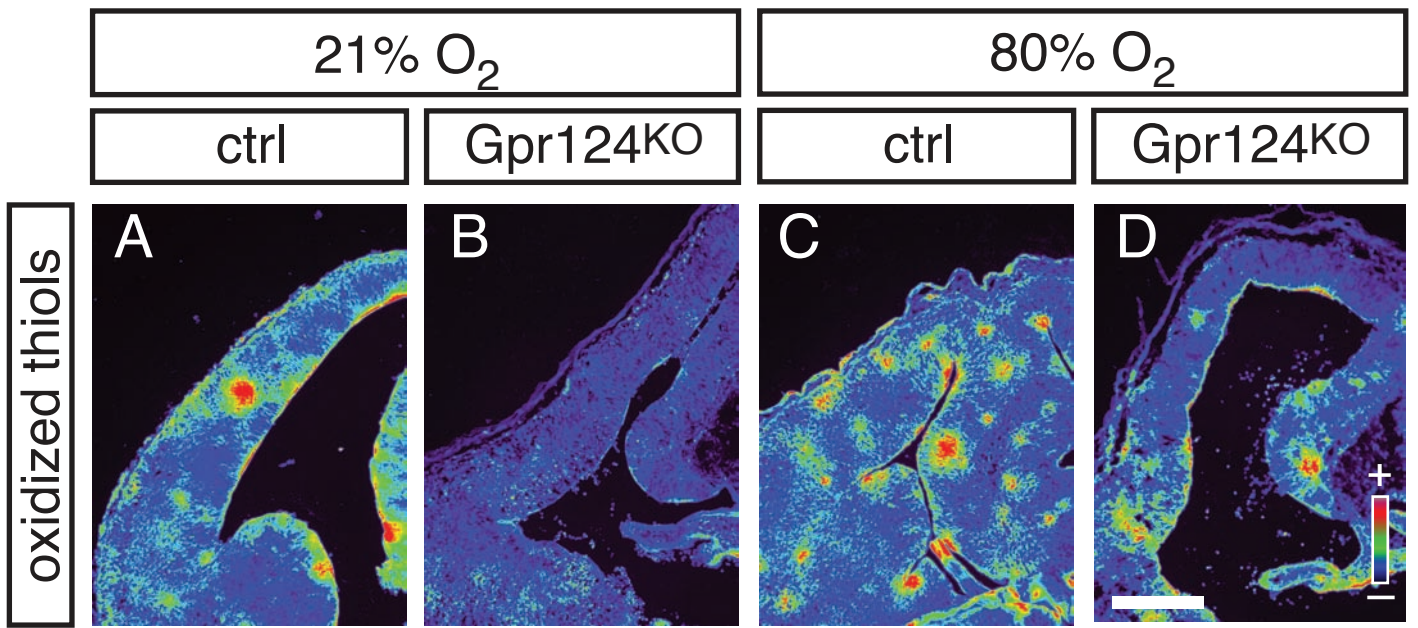
Appendix Figure S2



Appendix Figure S3



Appendix Figure S4



Appendix Figure S5

## APPENDIX

### APPENDIX FIGURE LEGENDS

#### APPENDIX FIGURE S1: SCHEME OF DIFFERENTIATION MARKER EXPRESSION

RGs can give rise to expanding and neurogenic RGs. Expanding RGs are devoid of differentiation marker expression, but can self-renew as well as generate neurogenic RGs that become committed to neuron production instead of expansion. Neurogenic RGs upregulate Tis21 (green nucleus) that is present in all neurogenic cells as well as Ngn1 (red circle in the nucleus) that is specifically abundant during the G1 phase of the cell cycle. Neurogenic RGs divide asymmetrically to generate one new neurogenic RG and a BP that upregulates its lineage marker Tbr2. BPs also express Tis21 and Ngn1 according to their cell cycle status.

#### APPENDIX FIGURE S2: HYPOXIA, APOPTOSIS AND CELL FATE CHANGES IN THE VZ OF GPR124<sup>KO</sup> EMBRYOS

**A,B**, Immunostaining for Glut1 in control (A) and Gpr124<sup>KO</sup> (B) cortices at E13.5. Asterisks denote meningeal blood vessels. **C,D**, Immunostaining for the hypoxia marker pimonidazole in control (C) and Gpr124<sup>KO</sup> (D) cortices at E13.5. **E-J**, Staining for EdU (E,G,H,J; red) and the BP marker Tbr2 (F,G,I,J; green) in the cortex of E13.5 control (E-G) and Gpr124<sup>KO</sup> (H-J) embryos, 8 hours after EdU injection. Note the reduced generation of EdU<sup>+</sup> Tbr2<sup>+</sup> BPs (yellow) in the VZ of Gpr124<sup>KO</sup> as compared to control embryos (G,J; arrows) that were generated from RGs at the apical surface within the last 8 hours. **K**, Quantification of EdU<sup>+</sup> Tbr2<sup>+</sup> BPs as a fraction of all EdU<sup>+</sup> VZ cells (mean±SEM; N=4; \*\* P<0.01). **L**, Quantification of TUNEL<sup>+</sup> cells (mean±SEM; N=5) in the cortex of E13.5 control and Gpr124<sup>KO</sup> embryos, showing no significant changes of

apoptosis upon inhibition of brain angiogenesis in *Gpr124*<sup>KO</sup> embryos. **M,N**, Quantification of *Ngn1*<sup>+</sup> *Tbr2*<sup>+</sup> BPs (M; mean±SEM; N=4) and *Tis21*-GFP<sup>+</sup> *Tbr2*<sup>+</sup> BPs (N; mean±SEM; N=4) expressed as % of all BPs in the VZ of E13.5 control and *Gpr124*<sup>KO</sup> cortices, showing no significant changes of neurogenic marker expression in BPs in control and *Gpr124*<sup>KO</sup> embryos. Dashed and dotted lines indicate the basal and apical boundaries of the VZ, respectively; full lines indicate the basal boundary of the cortex (A-J). N.S., not significant. Scale bar: 50 μm.

**APPENDIX FIGURE S3: LACK OF TRANSCRIPTIONAL ACTIVATION OF PROTOTYPICAL WNT- AND NOTCH-TARGET GENES IN *GPR124*<sup>KO</sup> NPCs**

**A**, Hierarchical expression cluster analysis of genes (rows) differentially expressed in VZ NPCs of wild type control (ctrl; left columns) and *Gpr124*<sup>KO</sup> embryos (right columns) at E13.5. A Row z-score of 0 indicates similar expression values across one row, while positive or negative Row Z-scores indicate increased or decreased expression, respectively, compared to the average expression value across the row. Histogram indicates distribution of z-scores for each gene shown. **B,C**, Quantification of relative mRNA expression levels, using RNA sequencing, of prototypical target genes of the Wnt pathway (B) comprising *Axin1*, *Axin2*, *Lef1*, *Tcf1*, and *Myc* or of the Notch pathway (C) comprising *Hes1*, *Hes5*, *Hey1*, *Hey2* in *Prom1*<sup>+</sup> NPCs from control and *Gpr124*<sup>KO</sup> cortices at E13.5 (mean±SEM; N=5). The expression levels were normalized to that in control NPCs for each gene. **D,E**, Quantification of relative mRNA expression levels of the same genes as shown in panels B,C in *Prom1*<sup>+</sup> NPCs from control and *Gpr124*<sup>KO</sup> cortices at E13.5 using quantitative RT-PCR (mean±SEM; N=4). The expression levels were normalized to that in control NPCs for each gene. N.S., not significant.



**APPENDIX FIGURE S4:** RECIPROCAL RELATION OF ANGIOGENESIS AND HIF TARGET GENE EXPRESSION IN THE DEVELOPING CORTEX

**A-I,** *In situ* hybridizations for the HIF-target genes *Pdk1* (A-C), *Bnip3* (D-F) and *Mct4* (*Slc16a3*) (G-I) at E10.5 (A,D,G), E11.5 (B,E,H) and E12.5 (C,F,I). Note the disappearance of expression matching the progression of angiogenesis (see Fig EV11-K). Arrows denote the border between the lateral and dorsal cortex. Scale bar: 200 $\mu$ m.

**APPENDIX FIGURE S5:** REGULATION OF TISSUE OXYGENATION BY HYPEROXIA TREATMENT MEASURED BY STAINING FOR OXIDIZED THIOLS

**A-D,** Staining for oxidized thiols in E13.5 control (A,C) and *Gpr124*<sup>KO</sup> (B,D) cortices after exposure of the pregnant dams to 21% O<sub>2</sub> (A,B) or 80% O<sub>2</sub> (C,D), showing increased tissue oxygenation in both control and *Gpr124*<sup>KO</sup> neocortices after exposure to 80% O<sub>2</sub>. Panels are pseudocolor conversions of staining intensity (from low [purple] to high [red]). Scale bar: 200 $\mu$ m.

## APPENDIX SUPPLEMENTAL MATERIALS AND METHODS

**MICROSCOPY AND IMAGING ANALYSIS:** Images were acquired on a Zeiss LSM 780 confocal microscope (Carl Zeiss), equipped with an EC Plan-Neofluar 10x/N.A. 0.30 M27, a Fluar 20x/N.A. 0.75 and an oil-immersion EC Plan-Neofluar 40x/N.A. 1.30 Oil DIC M27 objective (for Fig 1L,M,P,Q; Fig 2K,L; Fig 5E,F Fig 6H,I,M,N; Fig 7F-H,K-M; Fig EV4H-M) Alternatively a Zeiss LSM 510 Meta NLO confocal microscope (Carl Zeiss) with an EC Plan-Neofluar 10x/N.A. 0.30 M27, a Fluar 20x/N.A. 0.75 and an oil immersion EC Plan-Neofluar 40x/N.A. 1.30 Oil DIC M27 objective (for Fig 1F,G,I,j; Fig 2C,D,H,I; Fig 5B,C; Fig EV3E-G; Fig S1A,B,E-J) or a Zeiss LSM 710 confocal microscope (Carl Zeiss) with a C-Apochromat 40x 1.2 NA objective (for Fig EV1A-H,L-O; Fig EV2) was used for confocal imaging. ZEN software was used to acquire all confocal images. Epifluorescent imaging was performed using a Zeiss AxioPlan 2 Imaging microscope (Carl Zeiss) with a Plan-Neofluar 10x/N.A. 0.30 Ph1 and a Plan-Neofluar 20x/N.A. 0.50 objective, a AxioCam Hrc camera and the Axiovision software (for Fig1A,B; Fig2A,B; Fig4A-F,J-K; Fig EV3A-D,H-K; Fig EV4A-F; Fig S1C,D; Fig S3A-C,E,F,H,I) or a Leica DMI6000B microscope (Leica Microsystems) with a N Plan 5x/N.A. 0.12 or a HC PL Fluotar 20x/N.A. 0.50 objective, a DFC 365 FX camera, a DFC450C camera and the Leica AF image analysis software (for Fig 1C,D; Fig2E,F; Fig3H-I''; Fig4G-I''). Whole-mount brains of P5 pups (Fig 5J) were imaged using a Lumar.V12 stereomicroscope with a neolumar S 0.6x FWD 80mm objective and a AxioCam Mrc5. Image J (NIH) and Photoshop CS5 (Adobe) were used for adjusting image brightness and contrast and for generation of overlay images for the different channels and cell quantification.

For quantification of cell types in the VZ, SVZ and CP of the cortex, we used a combination of molecular markers together with cellular as well as nuclear morphology to establish these zones. We used immunostaining for the BP marker Tbr2, as the main

criterion to define the border between the VZ and the SVZ, because the SVZ is formed by continuous layers of Tbr2<sup>+</sup> BPs (Englund et al., 2005) while in the VZ, a minority of Tbr2<sup>+</sup> BP is intermingled with Tbr2<sup>-</sup> RGs. In stainings for Ki67 and EdU, we first took advantage of the difference in nuclear morphology between VZ and SVZ cells with elongated nuclei, aligned perpendicular to the ventricular surface in the VZ, while SVZ nuclei were more polygonal. Our second criterion was the intermingling of Ki67<sup>+</sup> with Ki67<sup>-</sup> cells in the SVZ that contrasted to the uniform labeling of VZ cells with Ki67. Together, the combination of both criteria allowed reliable identification of VZ versus SVZ cells.

The SVZ/IZ border was defined by different morphology of electroporated, GFP<sup>+</sup> cells in both zones. SVZ cells were polygonal with numerous thin processes, while IZ cells were elongated and oriented parallel to the ventricular surface. At the IZ/CP border, cellular morphology of electroporated, GFP<sup>+</sup> cells changed again, as CP cells could be identified as elongated, bipolar cells that are oriented perpendicular to the ventricular (and the basal) surface of the cortex. Another criterion for determining the SVZ was the dramatic increase in cell density from the IZ to the CP that was visible in nuclear counterstaining (not shown in the panels for clarity).

For quantification of RG differentiation in the VZ, all Hoechst 33248<sup>+</sup> cell nuclei were quantified in the VZ that was identified by co-staining with Tbr2, and the proportion of marker-positive (Ngn1<sup>+</sup>, *Tis21*-GFP<sup>+</sup> or Tbr2<sup>+</sup>) cells was expressed as a fraction of all VZ cells. Cells expressing two markers were quantified manually in overlay images. For Ki67/EdU colocalization analysis, all EdU<sup>+</sup> cells were quantified in a counting frame covering the entire cortex thickness and Ki67<sup>+</sup>/EdU<sup>+</sup> cells were quantified manually in overlay images. All images were acquired and quantified blinded to the genotype of the embryos or transfected plasmids.

For analysis of cell differentiation after in-utero electroporation, electroporated GFP<sup>+</sup> cells were quantified in the different cortical zones and expressed as fraction of all GFP<sup>+</sup> cells.

For each embryo or pup, at least 500 cells in 2-6 non-consecutive sections were counted.

For analysis of vascular area, 5 non-consecutive forebrain sections of 12  $\mu\text{m}$  thickness (covering the anterior-posterior axis) in each embryonic brain were stained for CD31 and Hoechst 33248 (Invitrogen) and imaged using a Zeiss Axioplan2 upright microscope. The area of the Hoechst<sup>+</sup> neocortex and the area of CD31<sup>+</sup> blood vessels within the neocortex above a predetermined threshold level quantified using Leica MM AF powered by MetaMorph<sup>®</sup> analysis software. Vascular area was expressed as a fraction of total cortex area.

For measurement of cortex size and thickness, 50  $\mu\text{m}$  sections from P5 brains were serially cut with a Vibratome (Leica VS 1200) and 5-6 sections with 250  $\mu\text{m}$  distance between each other, covering the medial and medio-caudal aspect of the cortex were stained with Hoechst 33248 (Invitrogen) in 12 well plates and imaged using the Leica DMI6000B microscope. The area of the cortical hemispheres and the thickness of the cortex were measured using Leica MM AF powered by MetaMorph<sup>®</sup> analysis software.

All images were acquired and quantified blinded to the genotype of the embryos or transfected plasmids.

**CELL-SORTING:** Neocortices were dissected from E13.5 embryos and single-cell solutions were prepared using the Neural Tissue Dissociation Kit (P) (Miltenyi Biotech) according to manufacturer's instructions. Prom1-positive cells were sorted by MACS using anti-mouse Prom1-microbeads (Miltenyi Biotech) according to the manufacturer's instructions. For FACS, dissociated cells from the cortices of E13.5 *Tis21-GFP*

heterozygous embryos were re-suspended in DMEM and GFP- and/or Prom1-positive cells were isolated using a FACSAria (BD Biosciences) set at purity mode and the appropriate sort rate (below 1000 cells per second for high purity and recovery of cells). Gating parameters were determined by side and forward scatter to eliminate debris, dead and aggregated cells and by green (530 nm) and far-red (635 nm) fluorescence to separate positive from negative cells (GFP-negative wildtype embryos). Less than 1% of non-fluorescent cells were included in the sort gate. Sorted cells were routinely re-sorted to determine their purity (95–98%). After sorting, an aliquot was removed to check for cell death revealing <5% of dead cells. Afterwards, the cells were centrifuged for 5 min at 400 x G and re-suspended in 300 µl of lysis buffer (RNA-link Mini Kit, Invitrogen) for RNA isolation. RNA was extracted using the PureLink RNA Mini Kit and On-column PureLink DNase treatment (Invitrogen), according to manufacturer's instructions.

**CELL CULTURE:** Neuro 2a (N2A) cells were maintained in Dulbecco Modified Eagle's Medium / Hams F12 supplemented with 10% fetal bovine serum, 1% non-essential amino acids, 2 mM glutamine, 100 U/ml penicillin and 10 µg/ml streptomycin (all from Life Technologies) and 1.6% NaHCO<sub>3</sub> solution (Sigma). Human embryonic kidney (HEK) 293T cells were maintained in Dulbecco Modified Eagle's Media supplemented with 10% fetal bovine serum, 2 mM glutamine, 100 U/ml penicillin and 10 µg/ml streptomycin (all from Life Technologies). Cells were routinely maintained in culture at 37°C, 5% CO<sub>2</sub> and 21% O<sub>2</sub> and transfected with Lipofectamine (Life Technologies).

Mouse neural stem cells (NSCs) were isolated from dissected E13.5 embryonic cortices by trituration of the tissue in ice-cold HBSS (Invitrogen) using fire-polished Pasteur pipettes. The cell suspension was passed through a 40 µm cell strainer (BD Biosciences) and centrifuged at 300xg for 4 minutes. The cell pellet is resuspended in full growth medium (Dulbecco Modified Eagle's Medium / Hams F12 supplemented with 2 mM glutamine, 100

U/ml penicillin and 10 µg/ml streptomycin, B27 (all from Life Technologies), 2 µg/ml Heparin (Sigma) and 20 ng/ml murine bFGF (Peprotech) and seeded in Petridishes (Corning) to grow neurospheres. Neurospheres were expanded up to 3 passages and at each passage used for experiments. For cell differentiation, single cell suspensions were made from neurospheres using Accutase (Sigma) and cells were seeded on coverslips (for immunocytochemistry (ICC)) or 24-well plates (for lactate measurement) that were coated with 1 µg/ml human recombinant laminin512 (Biolamina AB) overnight at 4°C. Cells were seeded at  $3 \times 10^4$  cells /cm<sup>2</sup> in full growth medium and cultured for two days to be either fixed for ICC or subjected to lactate measurement under proliferation conditions. For differentiation, after two days, medium was changed to differentiation medium I (full growth medium without Heparin) and for all following medium changes at two days interval, differentiation medium II (full growth medium without Heparin and bFGF) was used. Cells were either fixed or subjected to lactate measurement at 3 days or 7 days after onset of differentiation. For viral transductions, single cell suspensions were made from neurospheres using Accutase (Sigma) and cells were seeded on laminin-coated multiwell plates at a density of  $3 \times 10^4$  cells /cm<sup>2</sup> in full growth medium and transduced with lentiviruses at 2 hours after plating.

**LACTATE MEASUREMENT:** Cells were grown in 24-well plates and medium was aspirated on the day of measurement. 250 µl of the appropriate medium was added and cells were further cultured for 24 hours. Medium was collected and cells were lysed in 50 µl RIPA buffer (Sigma) per well. Cellular protein content was determined using the BCA assay (Pierce) according to the manufacturers recommendation. Lactate secreted into the medium was measured using a commercial Lactate assay (Trinity Biotech). 10 µl of conditioned medium or fresh medium as blank were incubated with 150 µl of assay buffer in a 96 well plate for 10 minutes at room temperature and the absorbance at 540 nm was compared to a lactate standard curve to calculate the amount lactate secreted into the

medium within 24 hours. The results were normalized to protein content.

**RNA-SEQ:** RNA from sorted Prom1+ cells was extracted using the Pure Link RNA Kit (Invitrogen) and genomic DNA was digested. RNA libraries were created using the Illumina TruSeq RNA sample preparation kit V2 according to the manufacturer's instructions. After confirmation of successful library construction, the resulting whole-exome libraries were sequenced on a HiSeq2000 (Illumina) using a V3 flowcell generating 1 x 50 bp reads. Raw sequencing reads were mapped to the transcriptome and the mouse reference genome (NCBI37/mm9) using TopHat 2.0 (Kim et al., 2013) and Bowtie2.0 (Langmead and Salzberg, 2012). On average 29,194,229 reads were assigned to genes with the HTSeq software package and normalized with EDASeq (Risso et al., 2011). Differential expression and appropriate p-values were calculated between all the individual pairs (control vs. knock-out) and between the control and knock-out group by DESeq (Anders and Huber, 2010).

**BIOINFORMATORIC ANALYSIS OF RNA-SEQ DATA:** Functional annotation clustering of the differentially expressed genes was performed using DAVID v6.7 (Hasan et al., 2013). Analysis for enrichment of transcription factor targets among the regulated genes was performed using ingenuity pathway analysis (Quiagen).

**MEASUREMENT OF TISSUE OXYGENATION:** Tissue oxygenation through oxidized thiol measurement was performed as described previously (Shah et al., 2011). Briefly, embryos were harvested in PBS with 100 mM N-ethylmaleimide (NEM) and 100 mM iodacetamide (IAA) (Sigma) to block reduced thiols. Embryo heads were then fixed in 4% paraformaldehyde containing 100 mM NEM and 100 mM IAA overnight and processed for cryosectioning. Oxidized thiols in 12 µm brain cryosections were reduced with 4 mM Tris(2-carboxyethyl)phosphine hydrochloride (TCEP) (Sigma Aldrich) in PBS for 30

minutes. Those reduced thiols were then labeled with 7-diethylamino-3-(4'-maleimidylphenyl)-4-methylcoumarin (CPM) (Sigma) for 30 minutes. After this step, labeling with Alexafluor-647-labeled Isolectin B4 (Invitrogen) was carried out as described (De Bock et al., 2013).

**MEASUREMENT OF MITOCHONDRIAL RESPIRATION:** Oxygen consumption rate (OCR) was measured using the extracellular flux analyzer XF24 instrument (Seahorse Bioscience Inc.). NSCs were plated, transduced with lentiviruses, and grown for 3 days in a Seahorse XF24 tissue culture plate. Then, the oxygen consumption rate was measured over a period of 2 minutes per measurement. In baseline conditions, 5 consecutive measurements of OCR are done. Next, the ATP synthase inhibitor oligomycin (Sigma), was injected to a final concentration of 1.2  $\mu$ M and 4 OCR measurements were performed. The drop in OCR reflects the oxygen consumption serving ATP production ( $OCR_{ATP}$ ).  $OCR_{ATP}$  was calculated by subtracting the average OCR after oligomycin injection from the average basal OCR. As a second injection, the complex III inhibitor Antimycin-A (Sigma) is added to a concentration of 1  $\mu$ M, resulting in abolishing the mitochondrial oxygen consumption, and the remaining, non-mitochondrial OCR was again measured four times. OCR corresponding to mitochondrial respiration ( $OCR_{MITO}$ ) was calculated by subtracting the average OCR after Antimycin A injection from the average basal OCR.

**PLASMIDS:** The following plasmids were previously reported: pcDNA3.1 (Invitrogen), pCMS-EGFP, pLVx (Clontech), pLKO (Sigma), pRL-TK (encoding Renilla Luciferase, Promega), pCAGGS-EGFP (Matsuda and Cepko, 2004) and 9xHRE::Luciferase (Aragones et al., 2008). 5'-accacatccagagccgaattgctc-3' or 5'-ggcaagaagtcccaatgcctg-3' shRNA sequences were cloned into pLKO or pLVx vectors to generate pLVx-Pfkfb3 (Pfkfb3 shRNA#1) or pLKO-Pfkfb3 (Pfkfb3 shRNA#2). 5'-acgcgctccggacgagactattga-3' shRNA sequences were cloned into pLVx to generate pLKO-scr or pLVx-scr (together



referred to as scr in the text), respectively. Murine wildtype HIF-1 $\alpha$  and HIF-1 $\alpha$  lacking the C-terminal activation domain (HIF-1 $\alpha$  $\Delta$ C) was cloned in frame with a T2A sequence and EGFP from pCMS-EGFP in the pCAGGS-EGFP vector to generate the HIF-1 $\alpha$  and HIF-1 $\alpha$  $\Delta$ C constructs, respectively, for in-utero electroporation. Murine wildtype HIF-2 $\alpha$  was cloned into pcDNA3.1 and used as a positive control for immunoblotting.

**IN-UTERO ELECTROPORATION:** Pregnant mice were isoflurane anaesthetized at E12.5 or E13.5, respectively and laparotomy was performed to expose the uteri. 1–2  $\mu$ l of PBS containing 2–4 mg/ml of plasmid was injected into the lumen of the embryonic forebrain followed by electroporation using 6 pulses of 35 V, 50 ms each at 1 s interval delivered through platinum electrodes using a BTX-830 electroporator (Genetronics) as previously described (Artegiani et al., 2012). After surgery, gestation was allowed to continue for an additional 3 days.

**EDU LABELING:** Pregnant mice were injected intraperitoneally with 5 mg/kg bodyweight EdU dissolved in sterile PBS, and embryos were collected after 8 hours or 24 hours and prepared for immunohistochemistry. EdU<sup>+</sup> cells in cryosections were detected using the Click-IT EdU Imaging Kit (Life Technologies) according to the manufacturers instructions.

**PIMONIDAZOLE LABELING:** Pregnant mice at E13.5 were injected intraperitoneally with 60 mg/kg bodyweight pimonidazole hydrochloride (Hypoxyprobe kit, Chemicon-Millipore, Billerica, MA, USA) dissolved in physiological saline, and embryos were harvested 90 minutes after injection. To detect the formation of pimonidazole adducts, embryonic brain cryosections were immunostained with Hypoxyprobe-1-Mab1 (Hypoxyprobe kit, Chemicon-Millipore, Billerica, MA, USA) following the manufacturer's instructions.

**LENTIVIRAL TRANSDUCTIONS:** Lentivirus production and lentiviral transductions were essentially performed as described (De Bock et al., 2013). Briefly, lentiviruses based on pLKO plasmid vectors (Sigma) and pseudotyped with vesicular stomatitis virus envelope proteins (VSV-G) were prepared in HEK 293 T cells as described (Carlotti et al., 2004) and used at a multiplicity of infection (MOI) of 30. Neural stem cells were transduced 2 hours after plating on adherent substrate for 2 days and then refed with full growth medium. Transduced cells were used in functional assays at 3 days post-transduction.

**TdT-MEDIATED dUTP-BIOTIN NICK END LABELING (TUNEL):** Apoptotic cells in 12  $\mu$ m-thick cryosections of embryo brains were visualized using the In Situ Cell Death Detection Kit, Fluorescein (Roche) according to the manufacturers instructions.

**IN-SITU HYBRIDIZATION:** Sense, and antisense riboprobes for Bnip3 (nt 641-1700 of NM\_009760.4), Pdk1 (nt 1282-2464 of NM\_133667.2) and Mct4 (nt 491-1568 of NM\_001038654.1) were DIG labeled by *in vitro* transcription (Roche) of cDNA encoding for their respective sequences. *In situ* hybridization on PFA-fixed embryo 20  $\mu$ m cryosections was carried out as described (Ruiz de Almodovar et al, 2011).

**LUCIFERASE ACTIVITY:** N2A cells were cotransfected with 9xHRE::Luciferase, phRL-TK and pCAGGS-EGFP, pCAGGS-HIF-1 $\alpha$ -T2A-EGFP or pCAGGS-HIF-1 $\alpha$  $\Delta$ C-T2A-EGFP, respectively. The cells were lysed and enzymatic luciferase activity was measured in a VICTOR X2 Multiplate reader (Perkin Elmer) using the Dual Luciferase Assay (Promega).

**IMMUNOBLOTTING:** For immunoblotting, protein samples were separated by SDS-PAGE and transferred to 0.45  $\mu$ m nitrocellulose membranes using the iBlot system (Life Technologies). For lysates, E13.5 mouse embryo forebrains were quickly dissected in ice-cold PBS and lysed in chilled lysis buffer (50 mM Tris-HCl pH 7.5, 150 mM NaCl, 0.1%

Triton-X100, 10% glycerol, 10  $\mu$ M MG132, 1% Complete protease inhibitor and 1% PhosSTOP (both from Roche), and centrifuged at 15,000g for 10 min at 4°C. For antibodies used in immunoblotting, see below. Antibody binding was detected using the Pierce ECL Western Blotting Substrate (Thermo) and luminescence signal was imaged using the ImageQuant LAS4000 instrument (GE Healthcare).

**ANTIBODIES:** The following primary antibodies were used: anti- $\alpha$ -Tubulin (Sigma, T 6199), anti-Brn2 (Santa Cruz, sc-6029), anti-CD31 (PharMingen-557355), anti-Ctip2 (Abcam ab18465), anti-Gfap (DAKO, Z0334), anti-GFP (Rockland, A11122), anti-Glut1 (Santa-Cruz, SC-1605), anti-HIF-1 $\alpha$  (R&D Systems, AF1935), anti-HIF-2 $\alpha$  (R&D Systems, AF2997), anti-Ki67 (abcam, ab15580), anti-Nestin (BD PharMingen, Cat# 556309), anti-Ngn1 (Santa Cruz, sc-19231), anti-Pax6 (Covance, PRB-278P), anti-Tbr1 (Abcam, ab31940), anti-Tbr2 (Abcam, ab23345), anti-Tubb3 (Promega, G7121).

**APPENDIX TABLE I: Used qRT-PCR assays**

<b>Gene symbol</b>	<b>Vendor</b>	<b>Assay code</b>
Prom1	IDT	Mm.PT.47.11320746
Fabp7	IDT	Mm.PT.47.10879959
Hes5	IDT	Mm.PT.47.7390739
Dcx	IDT	Mm.PT.47.7060296
Tubb3	IDT	Mm.PT.47.12543227
Glut1	AB Biosciences	Mm00441473_m1
Pdk1	IDT	Mm00554306_m1
Egln3	IDT	Mm.PT.51.11701105
Bnip3	AB Biosciences	Mm01275600_g1
Hif-1a	IDT	Mm.PT.51.8983770
NeuroD6	IDT	Mm.PT.47.17473417
Hk2	IDT	Mm.PT.49a.13201302
Eno1	AB Biosciences	Mm01619597_g1
Gapdh	AB Biosciences	Mm99999915_g1
Ldha	IDT	Mm.PT.49a.8242615
Pfkfb3	IDT	Mm.PT.51.6149366
Hprt	IDT	Mm.PT.42.12662529
Bact	IDT	Mm.PT.42.9990212.g

## SUPPLEMENTAL REFERENCES

- Anders, S., and Huber, W. (2010). Differential expression analysis for sequence count data. *Genome biology* *11*, R106.
- Aragones, J., Schneider, M., Van Geyte, K., Fraisl, P., Dresselaers, T., Mazzone, M., Dirkx, R., Zacchigna, S., Lemieux, H., Jeoung, N.H., *et al.* (2008). Deficiency or inhibition of oxygen sensor Phd1 induces hypoxia tolerance by reprogramming basal metabolism. *Nature genetics* *40*, 170-180.
- Artegiani, B., Lange, C., and Calegari, F. (2012). Expansion of embryonic and adult neural stem cells by in utero electroporation or viral stereotaxic injection. *Journal of visualized experiments : JoVE*.
- Carlotti, F., Bazuine, M., Kekarainen, T., Seppen, J., Pognonec, P., Maassen, J.A., and Hoeben, R.C. (2004). Lentiviral vectors efficiently transduce quiescent mature 3T3-L1 adipocytes. *Molecular therapy : the journal of the American Society of Gene Therapy* *9*, 209-217.
- De Bock, K., Georgiadou, M., Schoors, S., Kuchnio, A., Wong, B.W., Cantelmo, A.R., Quaegebeur, A., Ghesquiere, B., Cauwenberghs, S., Eelen, G., *et al.* (2013). Role of PFKFB3-driven glycolysis in vessel sprouting. *Cell* *154*, 651-663.
- Hasan, S.M., Sheen, A.D., Power, A.M., Langevin, L.M., Xiong, J., Furlong, M., Day, K., Schuurmans, C., Opferman, J.T., and Vanderluit, J.L. (2013). Mcl1 regulates the terminal mitosis of neural precursor cells in the mammalian brain through p27Kip1. *Development* *140*, 3118-3127.
- Kim, D., Pertea, G., Trapnell, C., Pimentel, H., Kelley, R., and Salzberg, S.L. (2013). TopHat2: accurate alignment of transcriptomes in the presence of insertions, deletions and gene fusions. *Genome biology* *14*, R36.
- Langmead, B., and Salzberg, S.L. (2012). Fast gapped-read alignment with Bowtie 2. *Nature methods* *9*, 357-359.
- Matsuda, T., and Cepko, C.L. (2004). Electroporation and RNA interference in the rodent retina in vivo and in vitro. *Proceedings of the National Academy of Sciences of the United States of America* *101*, 16-22.
- Risso, D., Schwartz, K., Sherlock, G., and Dudoit, S. (2011). GC-content normalization for RNA-Seq data. *BMC bioinformatics* *12*, 480.
- Shah, S.R., Esni, F., Jakub, A., Paredes, J., Lath, N., Malek, M., Potoka, D.A., Prasad, K., Mastroberardino, P.G., Shiota, C., *et al.* (2011). Embryonic mouse blood flow and oxygen correlate with early pancreatic differentiation. *Developmental biology* *349*, 342-349.

